Study of the effect of external periodic flow perturbations on heat transfer intensity in the impact jet

Bilsky A.V.*, Lozhkin Yu.A., Nebuchinov A.S.

S.S. Kutateladze Institute of Thermal Physics of Siberian Branch of RAS, Novosibirsk, Russia

Annotation

The aim of this work is to experimentally study unsteady heat transfer in an impact jet flowing onto a heated surface with the presence of large-scale structures and separated flows, as well as to search for possible mechanisms for controlling heat transfer by introducing external disturbances into the flow. In the work, a series of experiments was carried out to study an axisymmetric jet flowing normally onto a heated surface. The jet was both under natural conditions with different flow regimes and under external excitation at various frequencies and amplitudes. The instantaneous and average velocity and temperature fields in the near-wall part of the jet are measured using the PIV and PLIF methods. The correlations of velocity fluctuations and temperature fluctuations, which characterize the intensity of turbulent heat transfer, are calculated. It is shown that at different frequencies of external excitation of the jet, the intensity of turbulent transfer in the region of jet impingement on the wall changes. In the region of jet impingement on the wall, flow separation was recorded. It is shown that the interaction of the coherent structure with the wall leads to a local increase in the outflow of heat from the heated surface. The distributions of the heat transfer coefficient along the heated surface were also measured using a thermal imaging camera for various flow regimes, distances from the nozzle exit to the barrier, frequencies and amplitudes of the external flow disturbance. It is shown that when the jet is excited at different frequencies of the jet excitation, the heat transfer increases or decreases.

Keywords: heat exchange; impinging jet; PIV-method; PLIV-method

Designations

PIV ..... Particle Image Velocimetry
PLIF ..... Planar Laser Induced Fluorescence
Re..... Reynolds number
Nu..... Nusselt number
Sh..... Strouhal number
V, U..... Radial and longitudinal components of the average fluid velocity, [m/s]
U_0..... Average flow rate, [m/s]
f..... Frequency of external disturbances [Hz]
D..... Nozzle outlet diameter, [m]
h..... Distance from nozzle to impact surface, [m]
r..... Radial component of the coordinate system
q..... Heat flux [W/cm^2]
ν..... Kinematic viscosity of liquid, [m^2/s]

1. Introduction

The purpose of this work is to experimentally study unsteady heat transfer in an impact jet with large-scale structures and separated flows, as well as to search for possible mechanisms for controlling heat transfer by external perturbation of the flow. To solve this problem, optical methods for measuring instantaneous velocity fields (Particle Image Velocimetry - PIV) and instantaneous temperature

*Corresponding author
email: bilsky@itp.nsc.ru
doi: https://doi.org/10.23877/MS.TS.39.002
Published online: 15 June 2017

© Bilsky A.V., Lozhkin Yu.A., Nebuchinov A.S.

fields (Planar Laser Induced Fluorescence - PLIF) are used, as well as a thermal imaging method for measuring the intensity of heat transfer on a heated impact surface.

2. Measurement techniques PIV and PLIF

The PLIF method is based on the natural fluorescence of organic dye molecules excited by laser radiation. Intensity I of the light emitted by the dye per unit volume depends on the energy of the exciting light I_0, the quantum yield of the dye ϕ, light absorption coefficient of the dye ε and its concentration in solution C [3]:

$$I = I_0 C \phi \varepsilon \quad (1)$$

The concentration of the dye is assumed to be sufficiently low, and the attenuation of light as it propagates through the solution can be neglected. For a number of dyes, the quantum yield depends on temperature, which makes it possible to measure instantaneous temperature distributions in a flow. In field measurements, a pulsed laser is used to illuminate the flow cross section, from the beam of which a light knife is formed. Since fluorescence occurs at a longer wavelength than absorption, the light emitted by the dye can be separated from the laser light using a light filter and registered with a digital camera. By supplementing the installation with a second chamber and adding light-reflecting particles to the flow, it is possible to measure the velocity fields simultaneously with the temperature fields by the PIV method in the same flow section [3, 4]. The main sources of measurement error in the PLIF method are the instability of the laser pulse energy, the variability of its distribution along the beam, and the thermal noise of the camera. Procedures for processing instantaneous PLIF images should compensate for the influence of these factors in order to reduce the measurement error. The PLIF method and data processing procedures are described in more detail in [6].

3. Materials and methods

The experiment with an impact jet was carried out on an installation, which is a closed hydrodynamic circuit, consisting of a working section with an object under study, a pipeline system, a flow washer, a SAPPHIRE flow meter, a thermostat, a pump, a vibrator (Figure 1). When applying the PIV/PLIF method, the working fluid was a solution of the fluorescent dye Rhodamine B (Rhodamine B) in water (concentration 100 μg/L) with the addition of flow-monitoring polyamide particles (tracers) whose density is close to that of water. The total volume of the working fluid is 300 liters. The internal geometric dimensions of the working volume made of acrylic glass are 1 × 0.5 × 0.5 m.

The object of study is an axisymmetric submerged impact jet oriented vertically. The nozzle has a shape calculated according to the Vitoshinsky profile with a diameter at the nozzle exit D = 15 mm. To heat the impact surface, a heating element was created, which is a stainless-steel foil (thickness 0.125 mm, size 15 × 3 cm) glued to a "Textolite" base. The foil was heated using a programmable DC power supply with a power of up to 1000 W. Current setting accuracy (in current stabilization mode) ≈ 0.16 A. Temperature measurements on the heated surface were carried out using a FLIR Titanium 550M thermal imaging camera, which was mounted on top of the heater and recorded the temperature on the outer side of the heating element foil.

Flow disturbances were created using an electromagnetic vibrator. The vibrator created periodic flow fluctuations at the nozzle exit of a given amplitude and frequency. The vibrator voltage was set using a 12-bit DAC through a voltage divider and an amplifier. The supplied perturbations were assumed to be one-dimensional, since the entire mechanical vibration system was axisymmetric. An important condition for the experiment is the thermal stabilization of the entire hydrodynamic circuit. A constant temperature in the system was maintained using a thermostat using a resistance thermometer. Temperature was set with accuracy ≈ 0.1° C.

The measurements were carried out in the near-wall part of the jet using a combination of PIV/PLIF methods using the POLIS Stereo-PIV measuring system. The layout of the laser and cameras setup is shown in Figure 2. The measuring plane in the flow is illuminated by a double pulsed Nd:YAG laser.

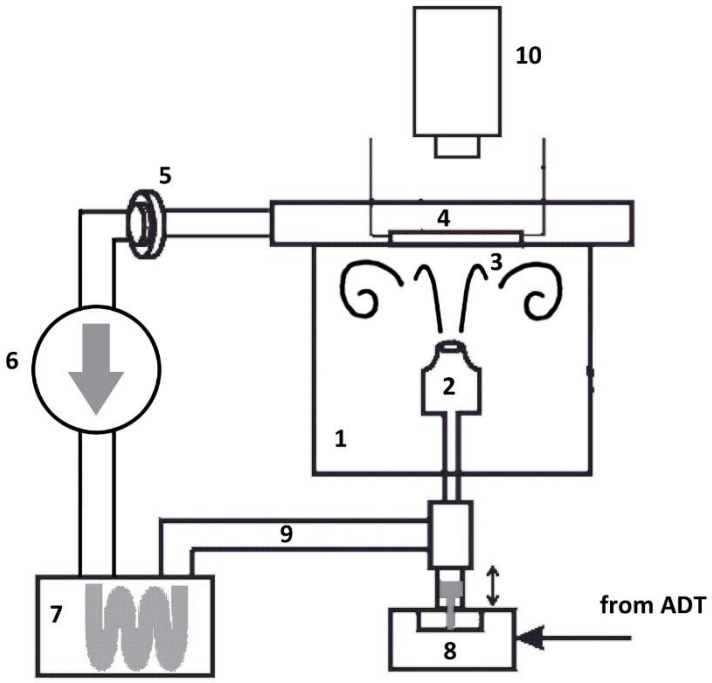

Figure 1. Scheme of installation with a thermal imager. 1 - working volume, 2 - Vitoshinsky nozzle (D = 15 mm), 3 - barrier, 4 - heating element, 5 - flow washer, 6 - pump, 7 - thermostat, 8 - source of external excitation - vibrator, 9 - pipeline, 10 - thermal imager

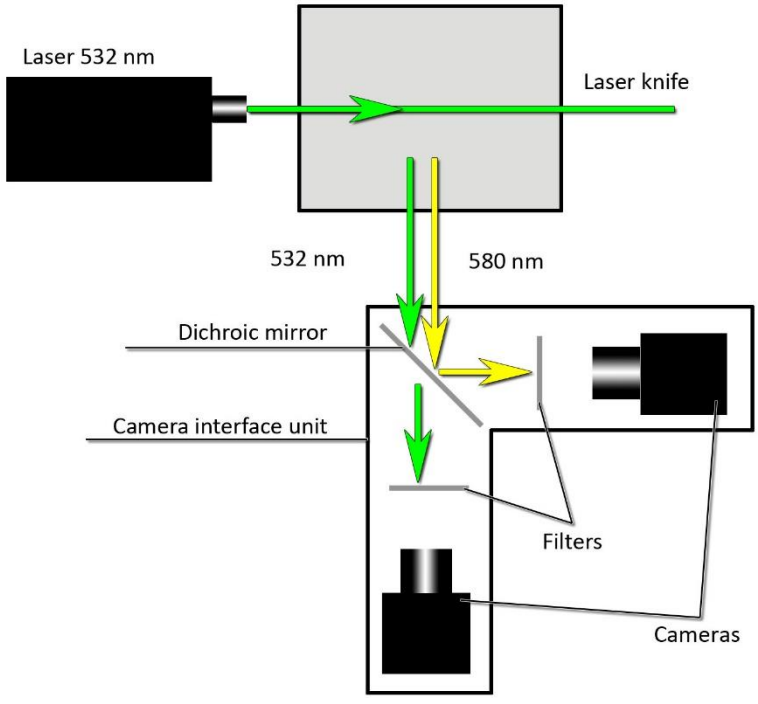

Figure 2. Scheme of PIV/PLIF system equipment installation (top view).

The distance from the near edge of the setup to the laser is. The opening angle of the laser knife is 3°. The thickness of the laser "knife" – 1 mm. The time delay between pulses is 184 μs. The laser radiation intensity was 50 MJ per impulse. Polyamide particles 20 μm in size and 1.05 g/cm^3 were used as tracers. The light scattered by the tracers and emitted by the fluorophore was separated using a dichroic mirror,

which reflects light with wavelengths greater than 540–550 nm and transmits light with shorter wavelengths. The light transmitted and reflected by the mirror was recorded by two digital cameras with appropriate light filters. To register one region of space with two cameras, the cameras were installed on a special interface device, as shown in Figure 2. The chambers were located on a metal base perpendicular to each other. The PIV camera is oriented so that the plane of its matrix is parallel to the plane of the laser knife. The cameras used (VideoScan 205-2001) allow recording two frames with a low (from 20 μs) delay, which is necessary for speed measurement by the PIV method. The bit depth of the ADC of the cameras is 10 bits.

The camera and laser were controlled from a computer using the ActualFlow software and the POLIS synchronizer, which synchronized the operation of the cameras and the laser.

The dynamic range of the measured velocities depends on the size of the elementary measurement area. In this experiment, a partition into regions of size was used, so the dynamic range is 80 (when using the iterative algorithm, it expands to 200). The measurement error of the instantaneous velocity field is 10%.

The accuracy of instantaneous temperature measurements using the PLIF method was ≈ 0.3° C.

4. Results and discussion

The work consisted of two parts. In the first one, the temperature distribution on the heated surface was measured using a thermal imager, which made it possible to calculate the distribution of the Nusselt number on the obstacle for various jet flow regimes, distances from the nozzle exit to the impact surface, and at different frequencies and amplitudes of the external flow disturbance. In these experiments, for each mode, 10.000 realizations of the instantaneous temperature were carried out, over which averaging was carried out. The heating element generated a constant heat flux q = 1.1 W/cm^2 in all studies using a thermal imager.

The first experiment in the first part was carried out in a jet with distances from the nozzle exit to the wall h/D = 1; 3. The experiment was carried out for various Reynolds numbers (Re = 2000-17400) without excitation.

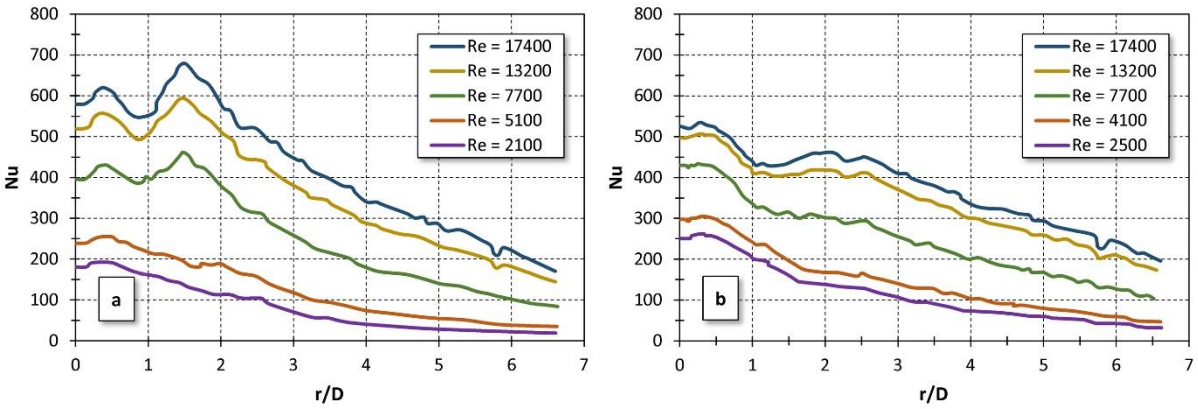

Figure 3. Distribution of Nu depending on Re; (a) h/D = 1; (b) h/D = 3

Figure 3 (a, b) shows the distributions of the Nusselt number (Nu) depending on the Reynolds number (Re) at the distance from the nozzle exit to the obstacle h/D = 1 and 3, respectively.

It can be seen that as Re increases, the heat transfer coefficient also increases under both conditions. Moreover, in the case of h/D = 3 (Figure 3(b)) in the center of the jet, a local minimum of the heat transfer coefficient is observed. In the area of large-scale vortices flowing onto the barrier ($r/D \approx$ 0.8), a maximum is observed. At high Re numbers, a secondary local maximum of the Nusselt number is observed, located at a distance of about 2 calibers from the nozzle axis ($r/D \approx 2$), the secondary maximum also becomes more pronounced and significant with an increase in the Reynolds number.

The hydrodynamic boundary layer near the wall remains laminar up to distances on the order of 1.5–2 nozzle calibers from the critical point. At these distances, the boundary layer becomes turbulent and, as a consequence, the heat transfer intensifies. In this region, a separated flow occurs near the wall, which is formed due to local positive pressure gradients induced by coherent structures. Such a heat transfer mechanism is described, for example, in [3].

In this work, the most intense heat transfer was observed in the region between large counter-rotating vortices. Further, as the distance from the nozzle axis increases, the heat transfer coefficient decreases monotonically.

At low Reynolds numbers, the distribution of the heat transfer coefficient changes its character. As *Re* decreases, the distribution of the heat transfer coefficient becomes more monotonous, decreasing the values with distance from the nozzle axis. This is observed in both cases.

A slightly different picture is seen in Figure 3(a) at a smaller distance from the nozzle exit to the impact surface ($h/D = 1$). The nature of the distribution of the Nusselt number changes. The secondary maximum is more pronounced and has a greater value than the primary, starting from $Re \approx 6000$.

The next experiment was carried out at different distances between the nozzle and the barrier ($h/D = 1 \div 7$ with a step $h/D = 1$), $Re = 10000$, without external excitation of the flow.

The graph (Figure 4) shows the characteristic distributions of Nusselt numbers depending on the distance to the obstacle.

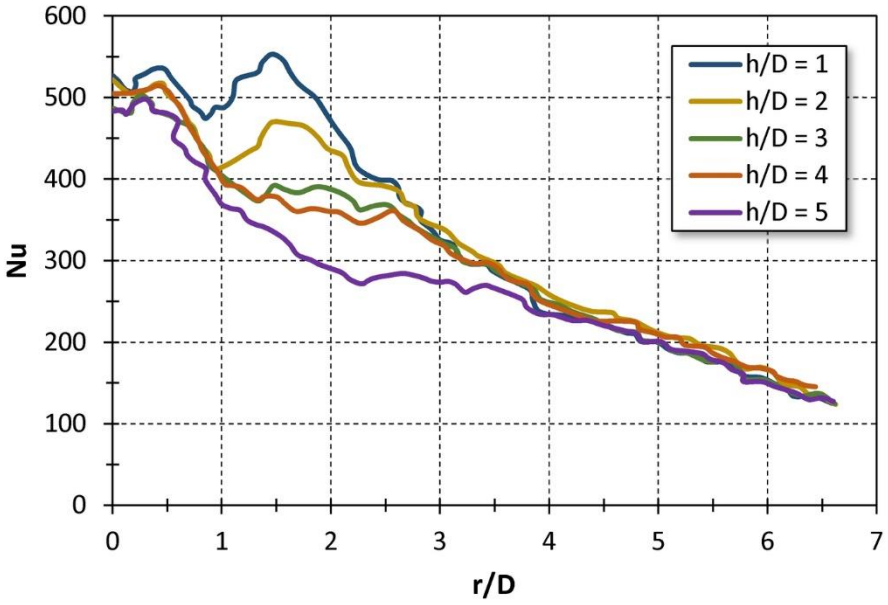

Figure 4. Distribution of *Nu* criterion depending on h/D; $Re = 10000$

It can be seen that at small distances from the nozzle exit to the wall ($h/D \le 4$), a local minimum is observed at the critical point. At distances $r/D \approx 0.8$, in the region where large-scale vortices flow onto the wall, a local maximum is observed. At distances $r/D \approx 2$, a secondary maximum of the heat transfer coefficient is observed, associated with turbulence of the boundary layer on the plate [5]. As the distance from the nozzle exit to the wall increases, the distributions of the heat and mass transfer coefficients take on a different form, decreasing monotonically as the distance from the critical point increases.

It can also be seen that the average heat exchange on the heating element decreases with increasing distance to it. Moreover, not in the entire area of jet impingement on the barrier, but in the flow separation zone ($r/D = 1 \div 4$), where the most intense suppression of Nu is observed. Since the jet, propagating in the medium at given distances to the barrier, almost does not lose its momentum, i.e., the velocity of the jet impinging on the impact surface at

the critical point does not change depending on h/D, then the heat transfer in the region of the critical point practically does not change.

The following shows the influence of the perturbation frequency on heat transfer (Figure 5). The Strouhal number values in the experiments were Sh = 0.4÷1; Sh = 1.3; Sh = 1.6; Sh = 2.

Figure 5(a, b) shows the most characteristic distributions of the heat transfer coefficient depending on the excitation frequency (f), expressed in the Strouhal number ($Sh = f \cdot D/U_0$). Expiration mode Re = 4000, distance between the nozzle exit and the heating element h/D = 1 (a) and h/D = 3 (b) with external flow disturbance frequencies Sh = 0.6 (f = 10.8 Hz), Sh = 0.9 (f = 16.2 Hz), Sh = 2 (f = 36 Hz).

At a small distance from the nozzle exit to the barrier (h/D = 1) with the introduction of external excitation of the jet, the heat transfer on the heated impact surface changes. Disturbing the flow at a frequency of Sh = 0.6 (f = 10.8 Hz), heat transfer is minimal, i.e., it is suppressed, and when disturbances are introduced, Sh = 0.9 (f = 16.2 Hz) is maximum, i.e., on the contrary, intensification is observed compared to the unperturbed state. At higher frequencies Sh = 2 (f = 36 Hz) the heat transfer coefficient behaves almost the same as without disturbance (Sh = 0). Moreover, all changes occur in the region up to $r/D \approx 3$. The difference between the minimum and maximum integral (that is, integrated over the area of jet leakage) values of the Nusselt number is ≈ 14.6%. And some change in the intensity of the secondary maximum at different perturbation frequencies indicates a change in the flow regimes in the separation region.

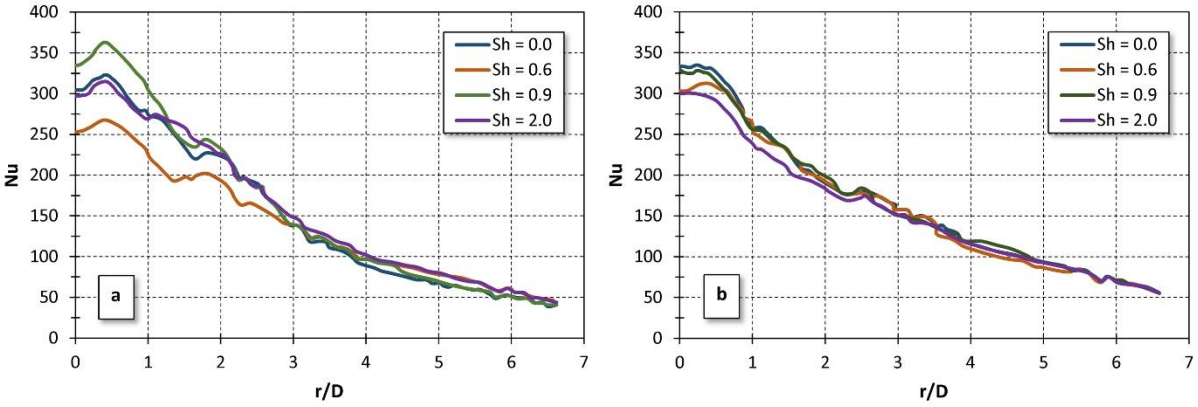

Figure 5. *Nu* distribution depending on *Sh*; *Re* = 4000; (a) h/D = 1; (b) h/D = 3

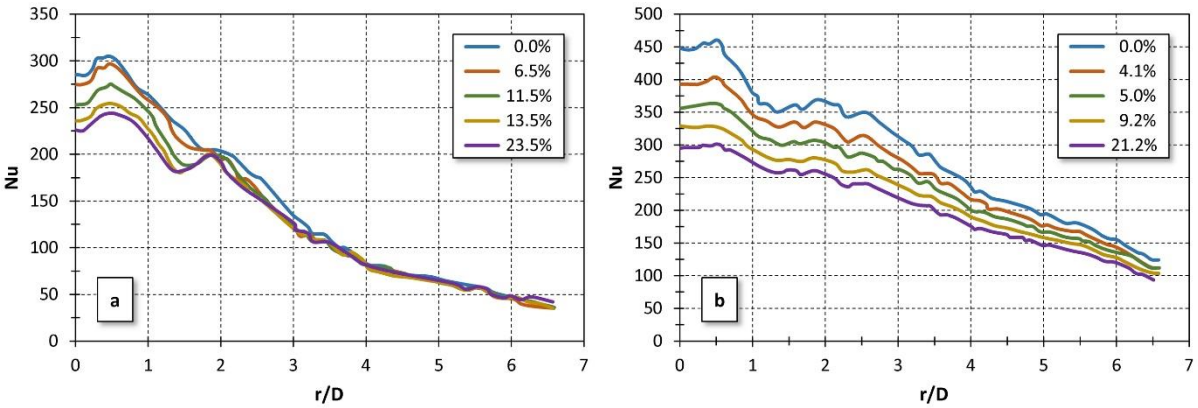

Figure 6. Distribution of *Nu* depending on the amplitude of external disturbances in % of the unperturbed state. h/D = 1, Sh = 0.6; (a) Re = 4000, (b) Re = 10000

At longer distances from the nozzle exit h/D = 3 Figure 5(b), the heat transfer on the heated surface remains practically unchanged. There is also no clearly expressed secondary maximum.

A similar picture is observed at Re = 10000.

In the next experiment, the influence of the amplitudes of the external disturbance of the flow on heat transfer was studied for two flow regimes Re = 4000; h/D = 1; Sh = 0.6; and Re = 10000; h/D = 3; Sh = 0.6. Figure 6 (a, b) shows the distributions of the Nusselt number depending on the excitation amplitude.

The heat transfer coefficient decreases with increasing amplitude. Since when external excitation of the jet at the frequency Sh = 0.6 is introduced, the effect of suppression of heat transfer on the impact surface is observed in both cases, this means that this effect increases with an increase in the amplitude of disturbances.

The second part of the work is devoted to a more detailed study of heat transfer processes in the leakage zone using a combination of PIV and PLIF methods. The instantaneous velocity and temperature fields in an axisymmetric submerged impact jet were simultaneously measured. In the experiment, for each mode, 2000 realizations of instantaneous velocity and temperature fields were measured, over which averaging was carried out.

To match the PIV and PLIF cameras, as well as to determine the scale factor, a spatial calibration was carried out. A calibration target with round markers (size d = 3 mm, distance between markers 3 mm) was placed in the area under study and filmed with two cameras simultaneously. Then, using calibration algorithms (similar to those used to calibrate the Stereo PIV method), the coordinate transformation and scale factor were calculated.

The measurements were carried out for the distance from the wall to the nozzle exit h/D = 3. The Reynolds number in the experiments was 4000, which corresponds to the average flow velocity at the nozzle exit U_0 = 0.27 m/s. Measuring area – the area of flow on the wall (from r/D = 0.4 to r/D = 3). The heating element emitted a constant heat flux q = 3.3 W/cm^2. the experiment was carried out for three cases of external excitation: an unperturbed case, and two perturbed ones - Sh = 0.5 (disturbance frequency f = 9 Hz), Sh = 0.9 (f = 16 Hz). Figure 7 shows the instantaneous velocity field obtained by processing images taken by the PIV camera. It can be seen that at a distance of about 2 calibers, there is a flow separation induced by a large-scale vortex structure located near and directed deep into the boundary layer.

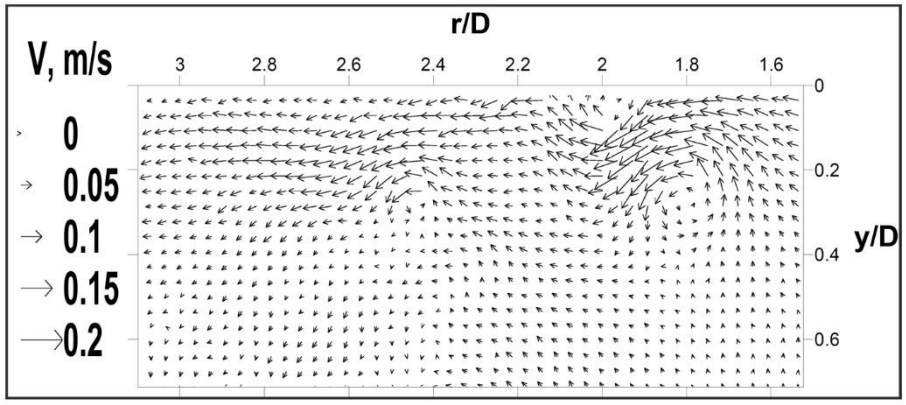

Figure 7. Instantaneous speed field. Re = 4000, h/D = 3

Figure 8 shows the instantaneous temperature field obtained by processing images taken by the PLIF camera. On instantaneous temperature fields, we observe local heat emissions. These surges can be associated with the presence of separated flows in the near-wall region, induced by large-scale structures near the wall. In [3], the most intense heat transfer was observed in the region between large counter rotating vortices. In this object, such a mechanism is also present in the regions between the main (coherent) vortex and the separated vortex of opposite vorticity sign.

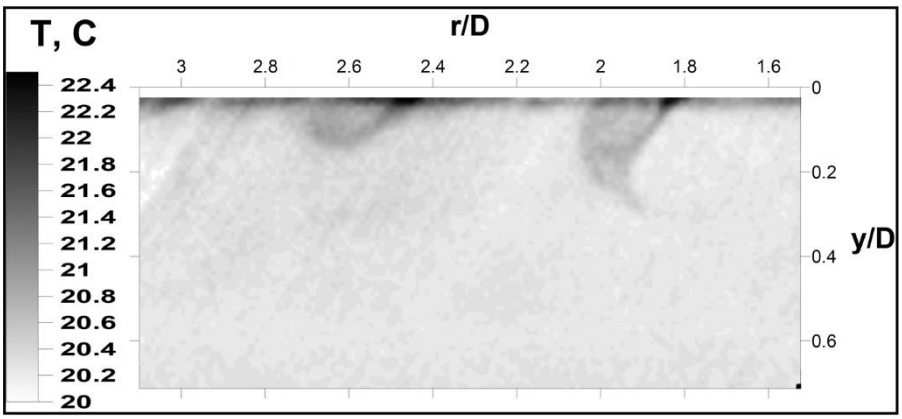

Figure 8. Instantaneous temperature field

This can be verified by superimposing the velocity field on the temperature field, which is shown in the following Figure 9. It can be seen that temperature spikes occur in those places where a large-scale vortex is observed. The vortex contributes to the entrainment of hot liquid from the wall, which increases the local heat transfer in this area.

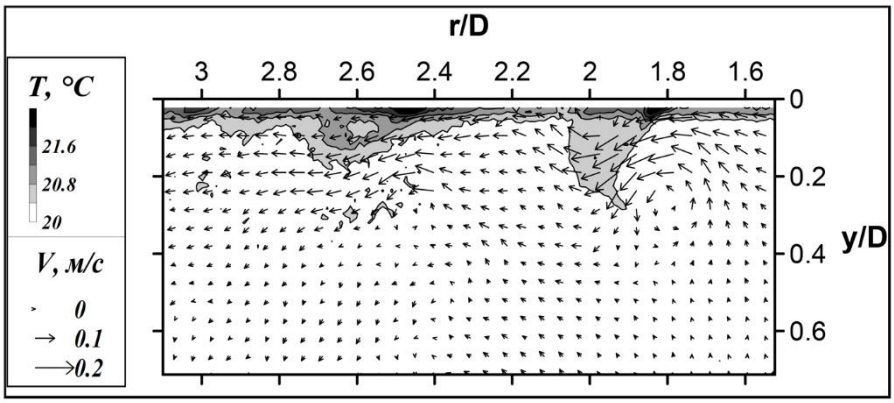

Figure 9. Instantaneous velocity and temperature fields

Figure 10 shows the correlations of temperature fluctuations with the normal component of velocity fluctuations <$t'V'$> for 3 different excitation modes: unperturbed case, with perturbation Sh = 0.5 and Sh = 0.9. Correlation values are normalized to the value $\rho \cdot C_p/Q$, where ρ – liquid density and C_p – heat capacity. It can be said that in the absence of a perturbation, the distribution of the correlation maxima is non-monotonous (discontinuous and with smaller absolute values), in contrast to the case with a perturbation. At a perturbation Sh = 0.5, the correlations begin to take on a more regular structure. And with a disturbance of Sh = 0.9, the correlation layer becomes more constant, expanding as it moves away from the nozzle axis. An increase in the absolute values of correlations in cases with an external disturbance of the flow means an increase in the role of the turbulent mechanism of heat transfer in the case of an external disturbance of the flow.

5. Conclusions

The object of study in this work was an axisymmetric impact jet flowing normally onto a heated surface. The jet was both in natural conditions and under conditions of external excitation of the flow at various Reynolds numbers, distances between the obstacle and the nozzle exit, frequencies and amplitudes of the external disturbance of the flow. The excitation frequencies corresponded to different modes of development of coherent structures and different values of the

intensity of the integral heat transfer on the wall.

The *Nu* distribution on the heated surface was measured for various regimes of jet outflow and regimes of external perturbation of the flow. It is shown that by introducing an external perturbation into the flow, it is possible to both enhance (at *Sh* = 0.9) and suppress (at *Sh* = 0.6) heat transfer in the area of the jet impingement, and the change in heat transfer intensity can reach 14.6%.

Simultaneous measurements of the velocity fields and temperature fields in the near-wall region of an axisymmetric turbulent jet flowing onto a heated surface are carried out. It is shown that the interaction of the coherent structure with the wall leads to a local increase in heat transfer from the heated surface. The correlations of velocity fluctuations and temperature fluctuations, which characterize the intensity of turbulent heat transfer, are calculated. It is shown that by varying the frequency of external excitation of the jet, it is possible to control the intensity of turbulent transfer in the area of jet impingement on the wall.

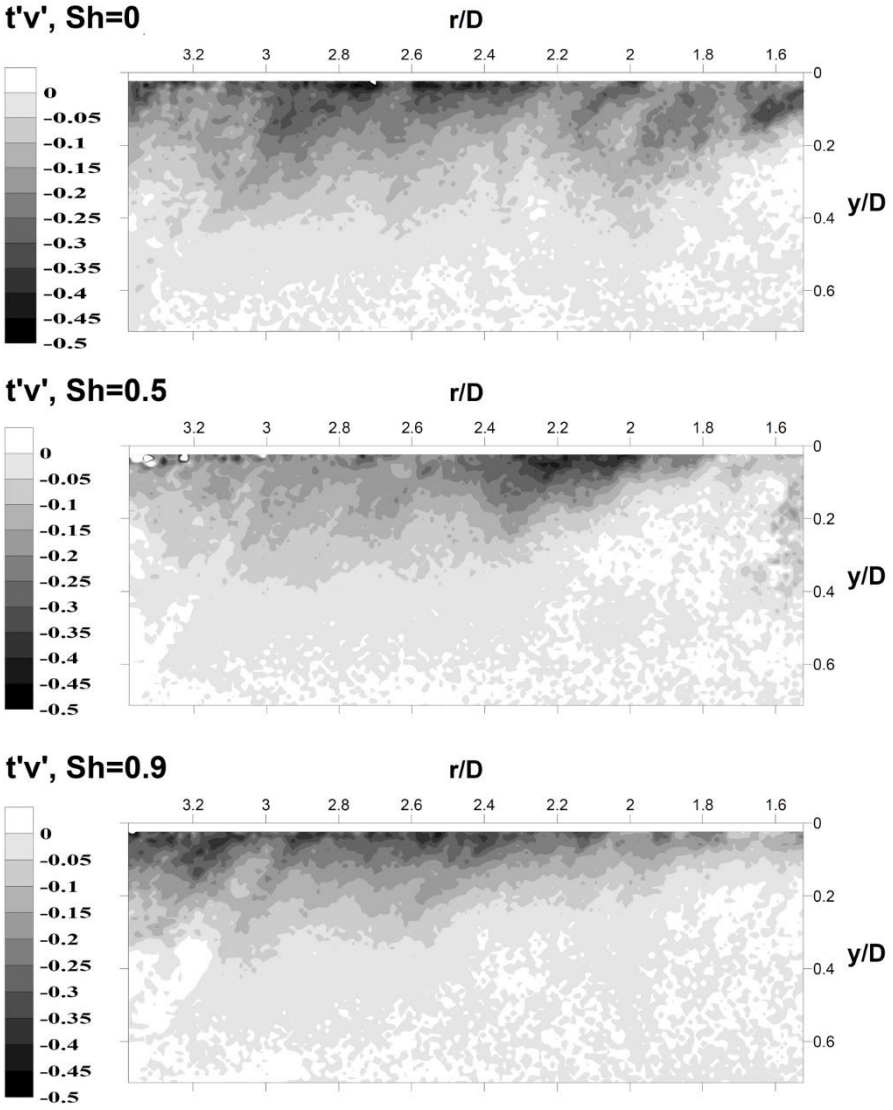

Figure 10. Correlations <*t'V'*>

References

[1] Liu T., Sullivan J.P. Heat transfer and flow structures in an excited circular impinging jet // International Journal of Heat and Mass Transfer. 1996. V. 39. № 17. P. 3695–3706.

[2] Raffel M., Willert C., Kompenhans J. Particle Image Fluorescence. A practical guide. Berlin: Sringer.

1998.

[3] Sakakibara J., Hishida K., Maeda M. Measurements of thermally stratified pipe flow using image-processing techniques // Experiments in Fluids. 1993. № 16. P. 82–96.

[4] Funatani S., Fujisawa N., Ikeda H. Simultaneous measurement of temperature and velocity using two-colour LIF combined with PIV with a colour CCD camera and its application to the turbulent buoyant plume // Measurement Science and Technology. 2004. № 15. P. 983–990.

[5] K. Kataoka Impingement heat transfer augmentation due to large scale eddies, Proc. 9th Int. Heat Transfer Conf., vol. 1, 1990.

[6] Bilsky A.V., Lozhkin Yu.A., Markovich D.M. PLIF Method for Studying Heat Transfer in Liquids // Ninth International Scientific and Technical Conference "Optical Methods for Investigating Flows". Proceedings of the conference. MPEI Publishing House: Moscow, 2007, pp. 406–409.